Fault Detection Method of Luojia1-01 Satellite Attitude Control System Based on Supervised Local Linear Embedding

ZHI QU[1,2,3], KAI XU[1,2,3], ZHIGANG CHEN[3], XIN HE[1,2], YANHAO XIE[3], MENGMENG LIU[3], FENG LI[3], AND SHUANGXUE HAN[3]

[1]Changchun Institute of Optics, Fine Mechanics and Physics, Chinese Academy of Sciences, Changchun 130033, China
[2]University of Chinese Academy of Sciences, Beijing 100049, China
[3]Chang Guang Satellite Technology Company Ltd., Key Laboratory of Satellite Remote Sensing Application Technology of Jilin Province, Changchun 130000, China

Corresponding author: Kai Xu (xukai118@126.com)

ABSTRACT This paper is aimed at the telemetry data of Luojia1-01 satellite attitude control system, and carries out the research on high-dimensional data feature extraction and fault detection based on supervised local linear embedding (SLLE). Because the general linear feature extraction method can not mine the feature information of nonlinear high-dimensional telemetry data, a data feature extraction and fault detection method based on local linear embedding is designed. Combined with the statistics SPE and T^2, the low-dimensional feature information is obtained for data statistics and monitoring faults. Due to the local linear embedded manifold learning method for the traditional batch processing mode is difficult to update and improve the database online, and the supervised local linear embedding method is introduced. The online sample feature extraction and fault detection schemes are designed, and the database is updated by updating the weight matrix through online samples. Finally, the effectiveness of the method is verified by Luojia1-01 satellite telemetry data. The results show that the fault detection method based on SLLE reduces the false alarm rate (FAR) by approximately 3% and the missing alarm rate (MAR) by approximately 10% compared with local linear embedding (LLE). This method effectively improves the detection capability of the anomalous state of Luojia1-01 satellite and has certain engineering application value.

INDEX TERMS Luojia1-01, telemetry data, fault detection, supervised local linear embedding (SLLE).

I. INTRODUCTION

On June 2, 2018, Luojia1-01 satellite developed by Wuhan University and Chang Guang Satellite Technology Co., Ltd. (Changchun, China) was successfully launched at the Jiuquan Satellite Launch Center. Luojia1-01 satellite is the first scientific experimental satellite used in nighttime imaging in China [1]–[4]. The Luojia1-01 satellite attitude control system ensures that the satellite adjusts its attitude according to mission requirements, thus ensuring the normal operation of satellite payload work and flight. The attitude control system will be in operation for a long time, and its high reliability is the basic guarantee for the entire satellite operation [5], [6]. According to statistics from the satellite fault database, 23%

of faults occur in attitude, orbit, and power systems, with the highest rate of failure. Once the attitude control system fails, the satellite will not be able to complete the scheduled function, or even lead to overall loss of control [7]. During the orbital operation, the Luojia1-01 satellite will transmit a large amount of telemetry data to the ground. These data truly reflect the satellite's payload and operating status. By mining the low-dimensional feature information of high-dimensional telemetry data, the satellite's abnormal state detection capability and reliability level can be effectively improved.

In Reference [8], Diagonal Recurrent Neural Networks (DRNN) is used to complete the satellite attitude control actuator fault diagnosis task, in which the actuator fault detection isolation uses different DRNN networks. Although it can be classified in real-time fault mode, the fault mode compatible with this method is very limited, and the

The associate editor coordinating the review of this manuscript and approving it for publication was Francesco Tedesco.

generalization ability is not ideal. In Reference [9], in order to realize the complex fault mode diagnosis of satellite attitude control system, the G2 based fault diagnosis technology is introduced, but how to build a complete expert knowledge base is a big problem. In Reference [10], [11], in order to realize the fault diagnosis under the redundant wheel condition of the satellite attitude control system, the synovial observer and the parameter estimation method are respectively used. This type of diagnosis method is called residual analysis method, Kalman filter, parity space, adaptive Methods such as the observer [12]–[15] are subject to this category. Although different quantitative methods can complete the fault diagnosis task to a certain extent, there are still problems to be solved. The observer method has higher requirements on the model and has no universality in the field of fault isolation. Parameter estimation can detect faults by estimating model parameters, but there is a problem that the fault detection delay time is long. In Reference [16], a machine learning/data mining (ML/DM) method is proposed, which can effectively detect the abnormal points in the telemetry data and combine the dynamic Bayesian network to realize fault diagnosis. In Reference [17], several methods for processing and anomaly detection of satellite telemetry data are summarized, such as parameter static threshold method, multi-threshold method and dynamic adaptive method. In Reference [18], using Principal Component Analysis (PCA) to extract satellite telemetry data feature information and reduce data dimension, combined with support vector machine (SVM) to achieve fault detection. The telemetry data returned by the satellite in orbit truly reflects the operating status of the system [19]. Through the analysis of the data, it can be judged whether the failure occurred or not. However, the analysis of telemetry data and the preparation for the later data-driven fault diagnosis are in the nascent stage, which is still immature, and many technical difficulties remain to be overcome.

Data-driven satellite fault diagnosis technology is still in its infancy, and research on telemetry data for attitude control systems is even rarer. During data mining and machine learning progress, satellite telemetry data is rarely used. Therefore, based on the above theory, the research on fault diagnosis technology of satellite attitude control system based on telemetry data analysis has certain exploration significance and engineering value.

II. CHARACTERISTICS ANALYSIS OF SATELLITE TELEMENTRY DATA

The telemetry parameters of the satellite are derived from various subsystems, and the data truly reflects the relevant operational status of each subsystem of the satellite. Due to the large amount of data, the fuzzy research and analysis of telemetry data is not targeted. For different research objectives, researchers need to use different telemetry data classification methods to facilitate data analysis and processing.
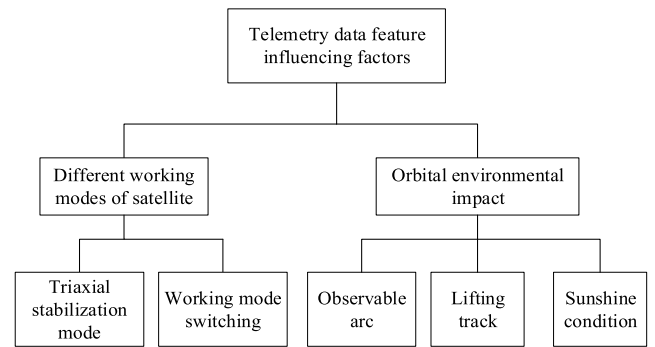

FIGURE 1. Analysis block diagram of influencing factors of telemetry data characteristics.

This paper mainly studies the telemetry data characteristics of the satellite attitude control subsystem.

Luojia1-01 satellite was launched into orbit in 2018 and is now in its orbit. The research and analysis of its telemetry data not only can understand the operational status of the satellite during its service, but also provide a powerful resource protection for satellite health management and life prediction. Through the detailed analysis of the characteristics of the telemetry data of Luojia1-01 satellite, the information detection technology is used to realize the anomaly detection of the satellite attitude control system. The influencing factors of the telemetry characteristic data of the satellite attitude control system are shown in Figure 1.

A. THREE-AXIS ATTITUDE STABLE WORKING MODE

Figure 2 shows the three-axis attitude angle and angular velocity telemetry data of the Luojia1-01 satellite received by the Wuhan University Satellite Ground Monitoring Laboratory from 9:30:11 to 9:40:17 on Dec 1, 2018. The real-time data of Luojia1-01 satellite is received every 2s, and the satellite ground monitoring laboratory receives 303 data, and the three-axis attitude angle of the satellite changes by about 0.3 degrees. It can be seen from the three-axis angular velocity telemetry data in Figure 2(b) that the three-axis attitude stable operation mode has a small range of satellite attitude angular velocity. When there is no special mission demand or emergency, the attitude of the satellite will be relatively stable under the adjustment of the attitude control system.

Satellite in orbit operation will inevitably encounter special circumstances, which means adjustment of working mode. The switching of different working modes implies a change in the state of the system, and the characteristics of the telemetry data also change. For the purpose of accomplishing similar attitude capture, spatial docking and attitude rollover tasks, the satellite needs to have a large angle maneuvering capability. At this time, the attitude data is different from the data characteristics under the three-axis stability. Therefore, the characteristics of satellite telemetry data in different working
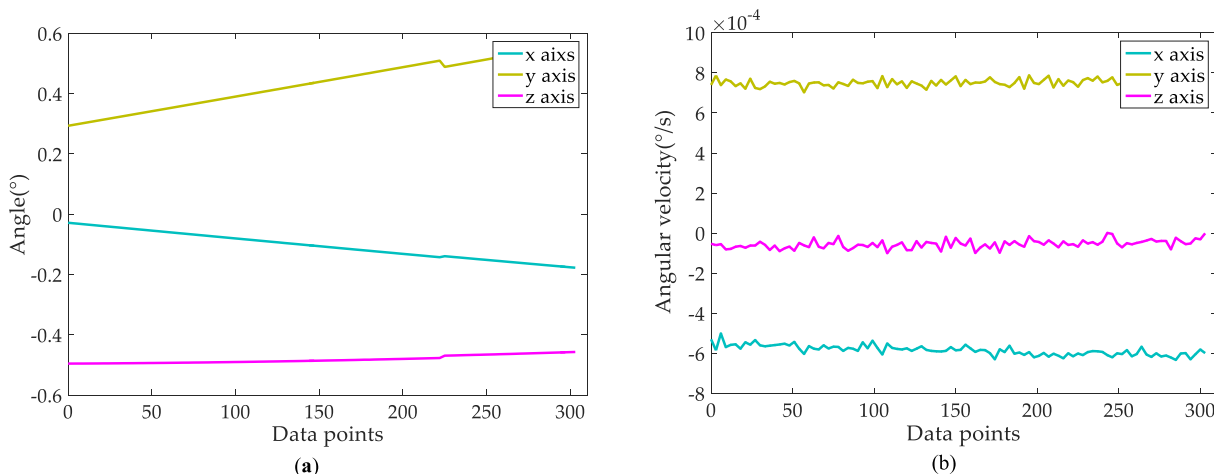
FIGURE 2. Attitude telemetry data in three-axis stable mode: (a) Attitude angle. (b) Angular velocity.
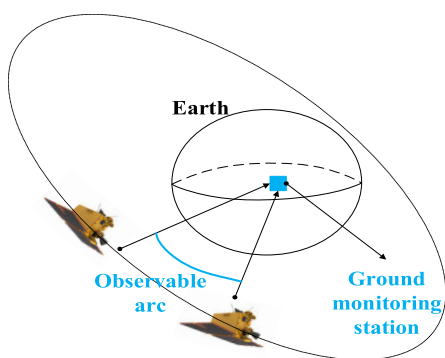

FIGURE 3. Schematic diagram of visible arc of ground monitoring station.

modes are different, and specific considerations are needed in practical applications.

B. OBSERVABLE ARC

During the orbital operation of the satellite, the telemetry data is transmitted back to the ground, and the ground monitoring station receives the data while carrying the mission of issuing satellite commands and missions. Only the satellite can run to the observable area of the ground station, then the telemetry data from the satellite can be received. The schematic diagram of the observable arc of the ground monitoring station is shown in Figure 3.

During the on-orbit operation of Luojia1-01 satellite, it will pass through the observable area of the satellite ground monitoring laboratory several times a day. At this time, the first system will send the relevant system information measured on the star back to the monitoring laboratory. From the schematic diagram of the observable arc of the ground monitoring station in Fig 3, it can be seen that the time of the satellite in each observable area passing through a certain ground station is limited, and the observable arc is only a small part of the entire satellite orbit, that is, each satellite transit the telemetry data that the ground station can receive

is the data between limited time period. Due to the relative motion of the satellite and the earth, the observation arc of the satellite each time passing through the same monitoring station is uncertain, there are differences in the way to enter the observation arc, the length of time, etc.

Figure 4 shows the telemetry data received on different dates of the Luojia1-01 satellite. The data curve shows that the time of passing through the Wuhan station is very short, about 8-10 minutes. The data points of the parameters are between 280 and 300.

C. SUNSHINE AND SHADOW AREAS

The satellite orbits the earth and cannot be kept in the sun. Changes in lighting conditions can have many effects on satellites: first, it affects the working state of the battery, that is, the satellite's energy system; secondly, the effects of different temperatures inside and outside the star, the lighting conditions and shadow conditions in space are different from the ground, and the temperature changes suddenly. The satellite itself is a big challenge, and each subsystem will behave differently in different areas. Taking the load current, battery voltage and bus voltage parameters on the Luojia1-01 satellite as an example, Figure 5 shows the telemetry data of the relevant variables received on Dec 1, 2018.

Under the light condition, the battery is in a state of charge, at which time the discharge current is near zero and the battery is not discharged. When the satellite is operating in the shaded area and the illumination is not received, the charging current is near zero and the battery is in a discharged state. It can be seen that different lighting conditions will bring different operating states within the system.

Through the analysis of the influencing factors of the above three aspects, it can be seen that the operational state of the satellite attitude control system will be affected by the on-board working mode, orbital characteristics and sunshine conditions. In other words, in order to analyze the characteristics of a parametric telemetry data in the satellite
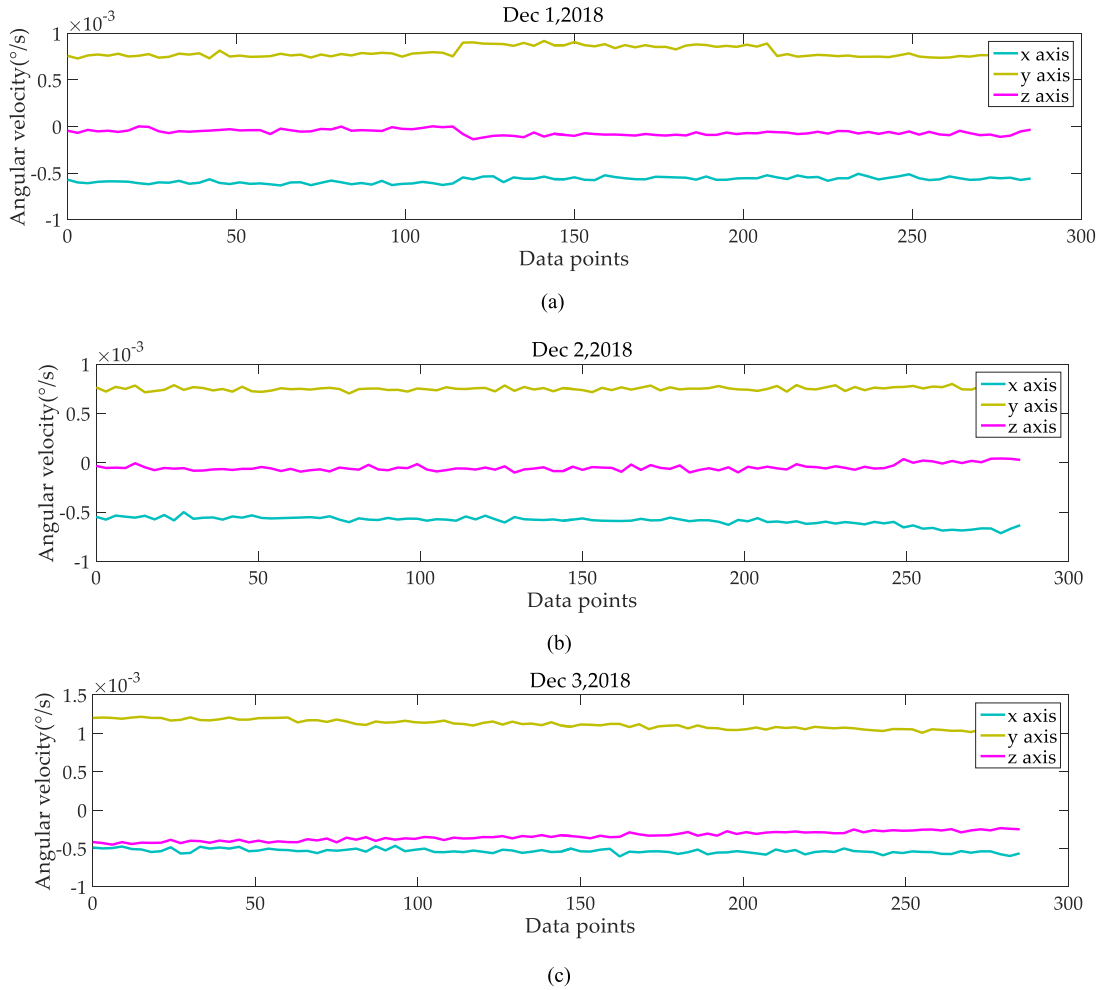
FIGURE 4. Attitude telemetry data received on different dates of the Luojia1-01 satellite: (a) Attitude angular velocity on Dec 1, 2018. (b) Attitude angular velocity on Dec 2, 2018. (c) Attitude angular velocity on Dec 3, 2018.

attitude control system, it is necessary to combine the working mode and the environment in which the satellite is currently operating.

III. TELEMETRY DATA PREPROCESSING

The telemetry parameters of the Luojia1-01 satellite attitude control system are many, and the telemetry data is not only large but also high in dimension. In the process of measurement, transmission and reception of telemetry data, it is inevitable to introduce various interference quantities or noises, which will have certain influence on data feature extraction and processing results. In order to ensure the accuracy of the later data feature extraction, the received high-dimensional telemetry data is first filtered to suppress noise to smooth the data.

With the improvement of digital signal processing technology and the updating of hardware devices, the traditional analog filter function can be realized with digital filters, and the digital filter is simple and has good performance. The digital filter can be divided into Infinite Impulse Response (IIR) and Finite Impulse Response (FIR). Both have problems:

the phase shift produced by the filtered data compared to the original data, the beginning of the filtered signal is distorted relative to the original data. To overcome the two problems, a zero-phase digital filter is used, and the schematic is shown in Figure 6.

Zero-phase digital filter theoretical description:

$$
\begin{aligned}
y_1(n) &= x(n) * h(n) \\
y_2(n) &= y_1(N - 1 - n) \\
y_3(n) &= y_2(n) * h(n) \\
y_4(n) &= y_3(N - 1 - n)
\end{aligned}
\tag{1}
$$

In Equation (1), $x(n)$ is input sequence, $h(n)$ is impulse response sequence of the filter, and $y_4(n)$ is output filtering result. To verify the filtering effect, a zero-phase digital filter is applied to the satellite attitude control system telemetry data. At present, the attitude angular velocity telemetry data in the three-axis attitude stabilization mode on Dec 1, 2018 is used, and the filter is used for filtering. The result is shown in Figure 7.
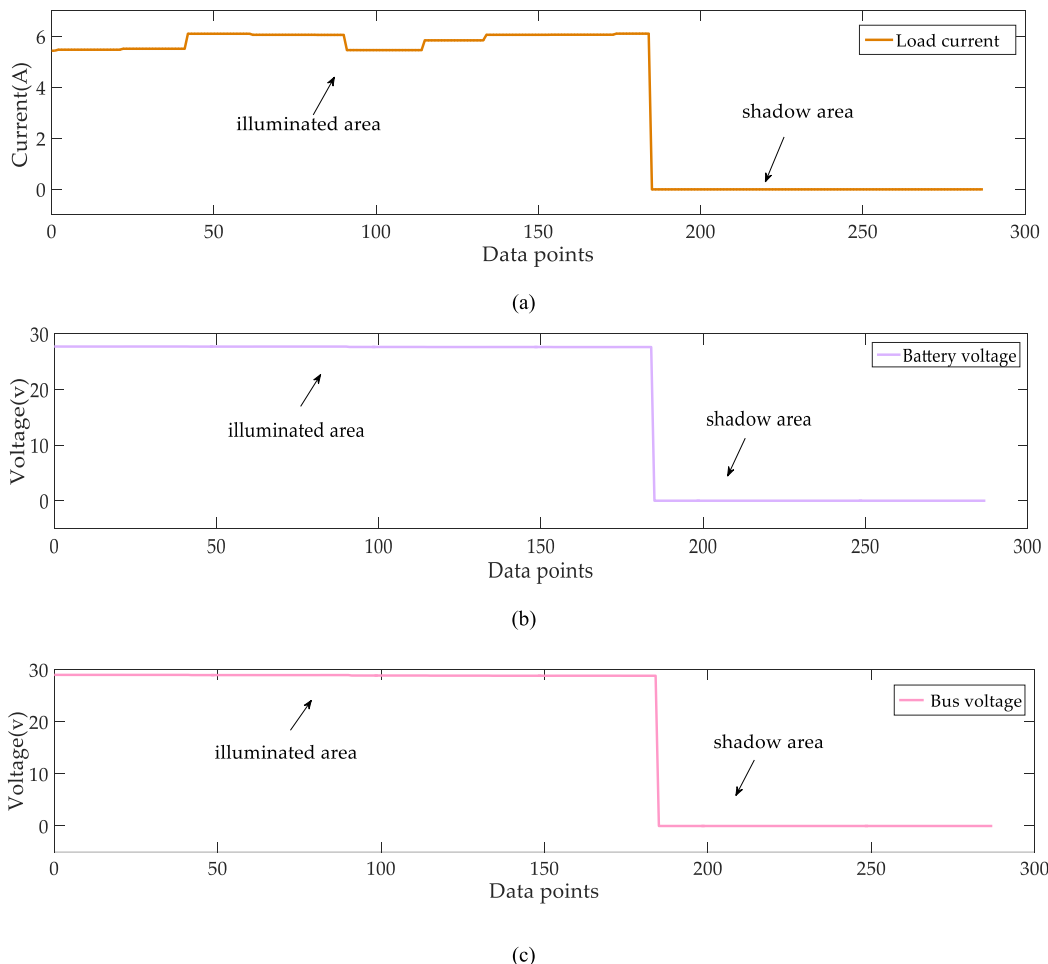
FIGURE 5. Relevant variable telemetry data received on Dec 1, 2018: (a) Load current telemetry data. (b) Battery voltage telemetry data. (c) Bus voltage telemetry data.
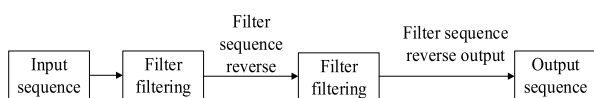

FIGURE 6. Zero-phase digital filter schematic.

As can be seen from the Figure 7, the zero-phase digital filter smooth the original data, removes the glitch in the data, and does not produce phase shift, maintaining the characteristics of the original data.

IV. THEORETICAL ANALYSIS OF LLE AND SLLE

A. PRINCIPLE AND ALGORITHM IMPLEMENTATION OF LLE

Local linear embedding (LLE) is a typical nonlinear manifold learning method while maintaining the intrinsic topology of the original data while achieving high dimensional data dimensionality reduction [20]. Different from other dimensionality reduction methods, LLE is described by local linear fitting to achieve global nonlinear structure. After each linear local dimensionality reduction, recombination results in a low-dimensional global representation.

Let the high dimensional input space be $X = \{x_i \in R^D, i = 1, 2, \cdots, N\}$, LLE algorithm aims to find the low dimensional embedded coordinates $Y = \{y_i \in R^d, i = 1, 2, \cdots, N\}, d < D$ of the original data X.

The implementation of LLE is divided into three steps:

Step1: Looking for neighborhood points

By calculating the Euclidean distance between each data point in the original high-dimensional data, the smallest k sample points of the sample point x_i are determined as the neighborhood point according to the distance. Let x_{ij} denote the *jth* neighborhood point x_j of data point x_i.

Step2: Reconstruction weight matrix

Calculating the reconstructed weight matrix W of the sample points by the neighboring points of the data point x_i, and minimizing the reconstruction error,

$$\min \varepsilon(W) = \left\| x_i - \sum_{j=1}^{k} w_{ij}x_j \right\|^2 \quad (2)$$

The optimization problem satisfies two constraints: first, x_i can only be reconstructed according to its neighborhood
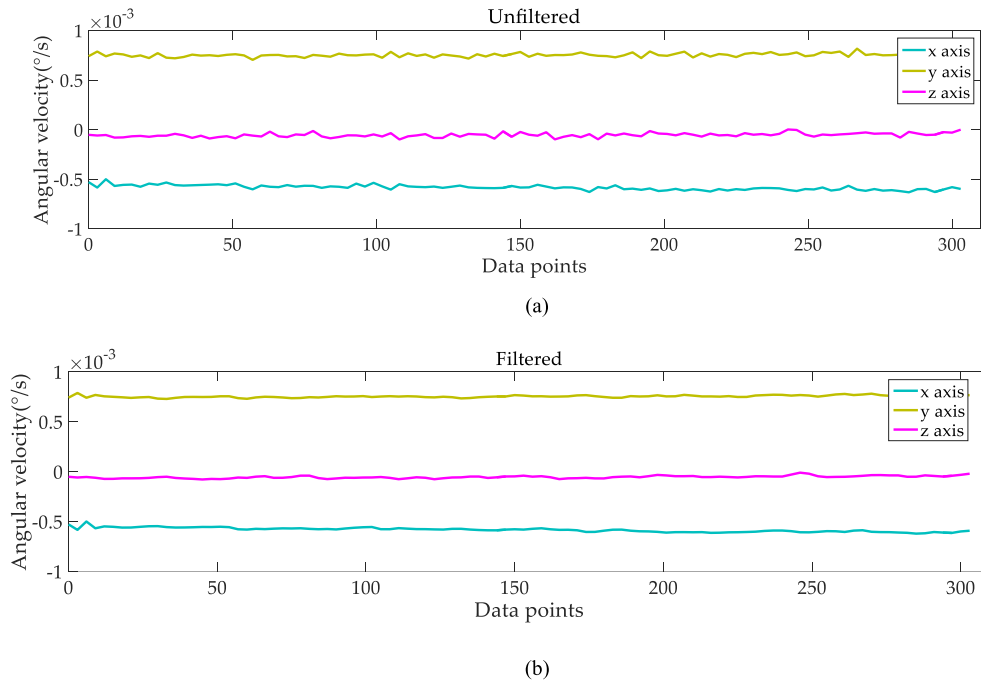
FIGURE 7. Attitude angular velocity telemetry data filtering curve: (a) Unfiltered telemetry. (b) Filtered telemetry.

points, x_j does not belong to the x_i neighborhood point, $w_{ij} = 0$; Second, the column vector of the weight matrix W must satisfy $\sum_{j=1}^{k} w_{ij} = 1$. At this point, the weight matrix can be solved by the least squares problem.

The above constraint $\sum_{j=1}^{k} w_{ij} = 1$ can be understood as a translation invariance from a geometrical point of view, that is, adding any vector c to the sample point x_i and its neighboring points does not have any influence on the reconstruction error.

$$x_i + c - \sum_{j=1}^{k} w_{ij}(x_j + c) = x_i + c - \sum_{j=1}^{k} w_{ij}x_j - \sum_{j=1}^{k} w_{ij}c$$

$$= x_i + c - \sum_{j=1}^{k} w_{ij}x_j - c$$

$$= x_i - \sum_{j=1}^{k} w_{ij}x_j \quad (3)$$

In order to solve the constrained solution of the formula $\min \varepsilon(W) = \left\| x_i - \sum_{j=1}^{k} w_{ij}x_j \right\|^2$, according to its translation invariance, we now assume $c = -x_i$, so there is

$$\left\| x_i - \sum_{j=1}^{k} w_{ij}x_j \right\|^2 = \left\| \sum_{j=1}^{k} w_{ij}(x_j - x_i) \right\|^2$$

$$= \left\| \sum_{j=1}^{k} w_{ij}z_j \right\|^2 = w_i^T zz^T w_i \quad (4)$$

In Equation (4), $z_j = x_j - x_i$, w_i is a $k \times 1$ vector, zz^T is a $k \times k$ symmetric matrix, called a (Gram) matrix, denoted as G_i, containing the inner product of all neighbors, that is, the minimum value that is transformed into the problem of (5).

$$RSS_i = \mathbf{w}_i^T G_i \mathbf{w}_i \quad (5)$$

Because of $\sum_{j=1}^{k} w_{ij} = 1$, there is (6).

$$L(w_i, \lambda) = w_i^T G_i w_i - \lambda \left(I^T w_i - I \right) \quad (6)$$

G_i is a symmetric matrix, and the partial derivative obtain:

$$\frac{\partial}{\partial w_i} L(w_i, \lambda) = 2G_i w_i - \lambda I = 0$$

$$\frac{\partial}{\partial \lambda} L(w_i, \lambda) = I^T w_i - I = 0 \quad (7)$$

That is $G_i w_i = \lambda I / 2$, where λ can be adjusted.

If $k > D$, that is, the neighboring point is larger than the sample dimension, the least squares of the above solution will have an infinite group solution. The usual solution is to perform L_2 adjustment, and the optimization problem is transformed into the following minimum solution problem:

$$\left\| x_i - \sum_{j=1}^{k} w_{ij}x_j \right\|^2 + \alpha \sum_{j=1}^{k} w_{ij}^2 \quad (8)$$

where $\alpha > 0$, the solution process is the same as the above process,

$$L = w_i^T G_i w_i + \alpha w_i^T w_i - \lambda \left(I^T w_i - I \right) \tag{9}$$

Then there is:

$$2G_i w_i + 2\alpha w_i - \lambda I = 0$$
$$2 \left(G_i + \alpha I \right) w_i = \lambda I \tag{10}$$

The weight matrix W can be solved.

Step3: Calculate low-dimensional embedded coordinates

Keep the weight unchanged, reconstruct the original data sample points in low-dimensional space, and minimize the reconstruction error.

$$\min \delta(Y) = \sum_{i=1}^{N} \left\| y_i - \sum_{j=1}^{k} w_{ij} y_j \right\|^2 \tag{11}$$

The constraints need to be met as follows:

$$\sum_{i=1}^{N} y_i = 0$$
$$1/N \sum_{i=1}^{N} y_i y_i^T = I \tag{12}$$

where I represents the $d \times d$ unit matrix.

$$\sum_{i=1}^{N} \left\| y_i - \sum_{j=1}^{k} w_{ij} y_j \right\|^2$$
$$= Y^T Y - Y^T (WY) - (WY)^T Y + (WY)^T (WY)$$
$$= ((I - W)Y)^T ((I - W)Y)$$
$$= Y^T (I - W)^T (I - W) Y \tag{13}$$

Define the "cost matrix" $M = (I - W)^T (I - W)$, that is $\sum_{i=1}^{N} \left\| y_i - \sum_{j=1}^{k} w_{ij} y_j \right\|^2 = Y^T M Y$, because $1/N \sum_{i=1}^{N} y_i y_i^T = I$, using the Lagrange multiplier factor:

$$L(Y, \mu) = Y^T M Y - \mu \left(N^{-1} Y^T Y - I \right) \tag{14}$$

Solving $MY = \frac{\mu}{N} Y$, it can be seen that Y must be the eigenvector of M. In summary, it can be seen that the last step of solving low-dimensional coordinates can be finally transformed into the eigenvector problem of solving matrix $M = (I - W)^T (I - W)$.

B. PRINCIPLE AND ALGORITHM IMPLEMENTATION OF SLLE

Dick [21] proposed a supervised local linear embedding algorithm (SLLE). In the first step, the traditional LLE algorithm searches for neighbors based on the Euclidean distance between sample points. While SLLE is processing this step, it adds category information for the sample points. The remaining steps of SLLE are consistent with the LLE algorithm. The SLLE algorithm mainly accomplishes two tasks

on the basis of LLE: first, how to update the original weight matrix W after introducing a new sample; second, the updated weight matrix is used to calculate low-dimensional coordinates, and for LLE, the eigenvector problem of transforming low-dimensional coordinate solution into sparse matrix M is solved. SLLE needs to solve how to find the updated sparse matrix.

Let the initial high-dimensional data be $X = \{x_i \in R^D, i = 1, 2, \cdots, N\}$, where k neighborhood points of a sample point x_i are represented as $\{x_{i(1)}, x_{i(2)}, \cdots, x_{i(k)}\}$, and the weight matrix corresponding to the reconstruction is denoted as W. The distance between the sample points x_i and x_j is denoted as Δ_i^j. Without loss of generality, assuming that the neighboring points described above have been reordered by distance, there is $\Delta_i^{i(1)} \leq \Delta_i^{i(2)} \leq \cdots \leq \Delta_i^{i(k)}$. For the new sample point x_{new}, the update algorithm of the weight matrix is as follows:

Step1: Calculate the distance between the new sample and each sample point in the original data, denoted as Δ_i^{new}, $i = 1, 2, \cdots, N$;

Step2: For any point x_i of this same point, if there is $\Delta_i^{new} < \Delta_i^{i(k)}$, then the neighborhood of this sample point needs to be updated to $\{x_{i(1)}, x_{i(2)}, \cdots, x_{i(k)}, x_{new}\}$, and then the neighboring points are sorted in ascending order according to the distance between the neighboring point and the sample point, which is $\{x'_{i(1)}, x'_{i(2)}, \cdots, x'_{i(k+1)}\}$;

Step3: It is only necessary to calculate the weight vector w_i corresponding to the sample point x_i in which the neighborhood point region changes, and then the weight matrix W is updated accordingly, and the weight vector of the sample point is calculated by referring to formula (2) to formula (10).

It can be seen that in the SLLE algorithm, the update of the weight matrix is mainly performed on samples whose neighborhood points change. In other words, when a new sample has an impact on the neighborhood of one or more sample points in the original database, then SLLE will update the neighborhood features and weight vectors of those sample points accordingly. In this way, the information redundancy caused by introducing all new samples into the database can be avoided, and the calculation of the algorithm only needs to update the weight vector of a small number of sample points, thereby reducing the calculation cost. After the new sample is added, the new $(N + 1) \times (N + 1)$ weight matrix W' is obtained accordingly, and the latest "cost matrix" M can be solved, and the corresponding low-dimensional embedded coordinates represent Y' after the new sample is introduced.

In this paper, SLLE focuses on database updates on sample points of neighborhood feature changes, saves resources and takes less time, and only updates those important samples that have an impact on the internal structure of the database. On the one hand, it can guarantee the completeness of the database. On the other hand, it can avoid information redundancy.

TABLE 1. Telemetry data schedule for feature extraction.

Data sources	Date	Telemetry parameter	Number of samples	Task mode
Luojia1-01 satellite attitude control system telemetry data	Dec 1, 2018- Dec 3, 2018	Magnetic torque current; Flywheel torque; Fiber optic gyro angular Velocity; Attitude angular velocity	1220	Three-axis Attitude Stable Working Mode

V. TELEMETRY DATA FEATURE EXTRACTION AND FAULT DETECTION

In this section, the telemetry data of the Luojia1-01 satellite attitude control system is taken as the research object. The low-dimensional embedded feature information of high-dimensional telemetry data is extracted by LLE manifold algorithm and SLLE manifold algorithm respectively, combined with statistics *SPE* and T^2 for low-dimensional features. Information implementation fault detection [22].

A. SPE STATISTIC

The *SPE* statistic is mainly used to describe the model residual space or the noise in the process information. For an online updated sample data x_{new}.

The corresponding *SPE* calculation formula is as follows:

$$SPE_{\text{new}} = \left\| x_{\text{new}} - \hat{x}_{\text{new}} \right\|^2 \tag{15}$$

where $\hat{x}_{new} = A^T A x_{new}$ represents the reconstructed estimate of the sample point x_{new}.

The distribution of the corresponding statistic *SPE* with a control limit that is approximately satisfied can be expressed as follows:

$$SPE_\alpha = \theta_1 \left[\frac{c_a\sqrt{2\theta_2 h_0^2}}{\theta_1} + 1 + \frac{\theta_2 h_0(h_0 - 1)}{\theta_1^2} \right]^{1/h_0} \tag{16}$$

In Equation (16), λ_j is eigenvalues of covariance matrices; $h_0 = 1 - 2\theta_1\theta_3/(3\theta_2^2)$, $\theta_i = \sum\limits_{j=i+1}^{m} \lambda_j^i, i = 1, 2, 3, c_\alpha$ is the normal distribution value at the confidence level c. When SPE_{new} is smaller than the control line SPE_α, the system is operating normally.

B. T² STATISTIC

T^2 statistic is used to describe the degree of change of the sample in the model space. For an online updated data x_{new}, its low-dimensional embedding is y_{new}, and its calculation formula is as follows:

$$T_{new}^2 = y_{new}^T \Lambda^{-1} y_{new} \tag{17}$$

where Λ is the covariance matrix of the low-dimensional embedded coordinates Y of the offline training data, $\Lambda = \frac{YY^T}{N-1}$.
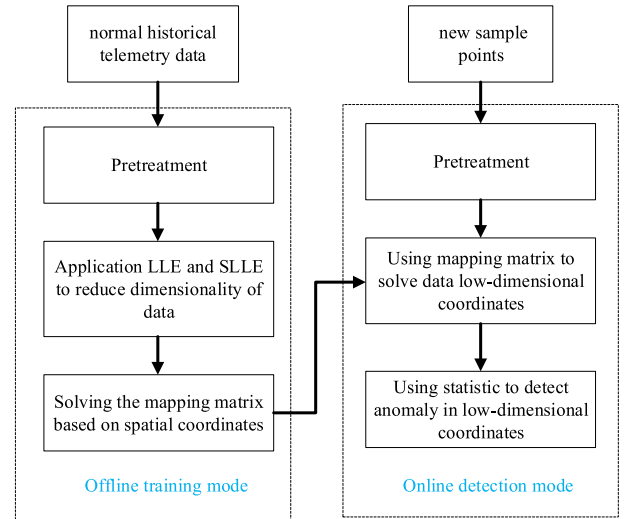

FIGURE 8. Fault detection algorithm flow chart.

The control limit of T^2 conforms to a certain distribution, and the specific representation is as follows:

$$T_\alpha^2 = \frac{\alpha (N^2 - 1)}{N(N - \alpha)} F_\alpha(\alpha, N - \alpha) \tag{18}$$

In Equation (18), α is the confidence level, and $F_\alpha(\alpha, N - \alpha)$ is the F distribution of the degrees of freedom $\alpha, N - \alpha$. When the T^2 statistic value of the sample exceeds the corresponding statistical control limit, the sample point is abnormal, otherwise it is normal.

The normal satellite attitude control system telemetry data is trained, and the low-dimensional embedded space is obtained by LLE and SLLE algorithm, so that the high-dimensional data space to the low-dimensional embedded space mapping matrix is obtained, and then the mapping matrix is used to obtain the low of the online sample points. Dimensional feature space, and finally combined with statistics for fault detection tasks, the flow shown in Figure 8.

In order to further illustrate the algorithm feature extraction process, the selected telemetry data of the Luojia1-01 satellite attitude control system is: from Dec 1, 2018 to Dec 3, 2018, there are 12 telemetry parameters. The telemetry data is the daily falling orbit data. For details, see the telemetry data list used in the feature extraction in Table 1.

VI. ALGORITHM APPLICATION

Since the existence of interference noise and the dimension of the telemetry parameter are different, before applying the
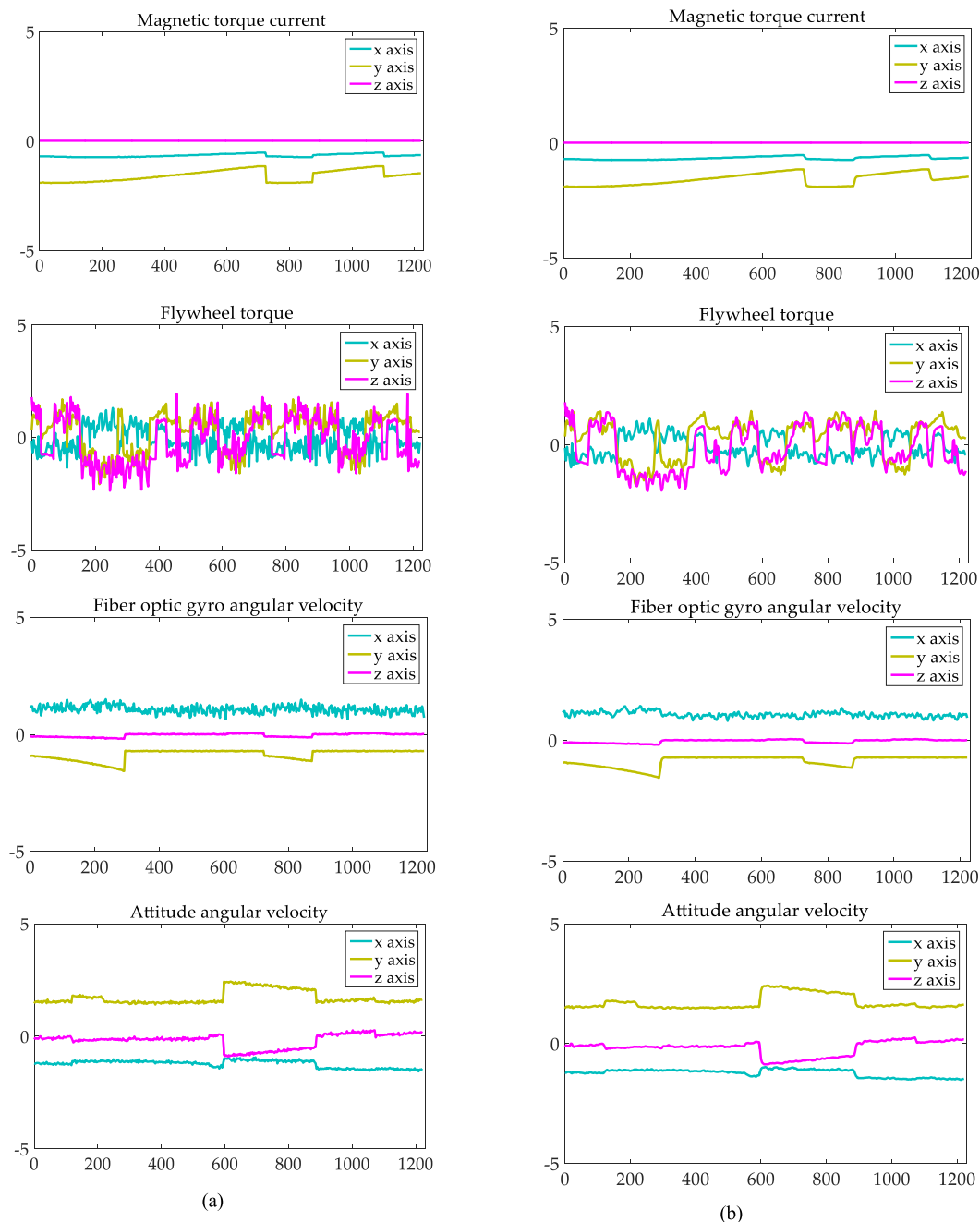
FIGURE 9. Telemetry data before and after pre-processing: (a) Unfiltered telemetry: Magnetic torque current; Flywheel torque; Fiber optic gyro angular velocity; Attitude angular velocity. (b) Filtered telemetry: Magnetic torque current; Flywheel torque; Fiber optic gyro angular velocity; Attitude angular velocity.

LLE and SLLE algorithms to extract the feature information of the high-dimensional data, the telemetry data must be preprocessed as follows: the wild value, the smoothing filter, and unified dimension. The telemetry data before and after preprocessing is shown in Figure 9.

The left side is the original signal after the unified dimension, and the right side is the pre-processed data. Telemetry parameters are magnetic torque current, flywheel torque, fiber optic gyro angular velocity and attitude angular velocity.

The LLE algorithm is used to reduce the dimension and feature extraction of the preprocessed data, and the parameters are taken $d = 3$, $k = 60$.

Figure 10 shows the data after pre-processing and LLE dimensionality reduction. Figure 10(a) shows the telemetry data after the original preprocessing, and Figure 10(b) is the dimensionally reduced data. The dimensionality reduction data retains the main features in the original data. The LLE algorithm mines the feature quantity
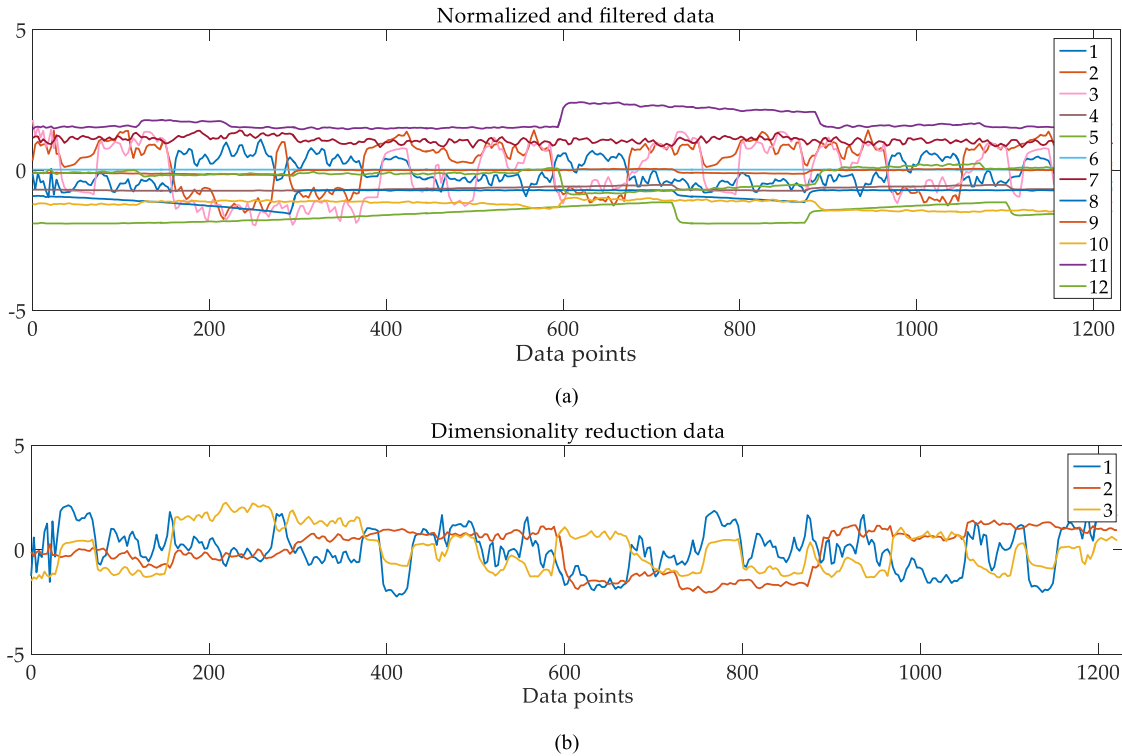
FIGURE 10. Telemetry data dimensionality reduction results: (a) Normalized and filtered data: 1,2,3- magnetic torque current; 4,5,6-flywheel torque; 7,8,9-fiber optic gyro angular velocity; 10,11,12-attitude angular velocity. (b) Dimensionality reduction data.

of the data in the dimension reduction process of high-dimensional data, and the fault diagnosis essence is a process of identifying the abnormality. If the LLE algorithm is applied to the fault telemetry data of the satellite, the feature extraction must transfer the fault information in the high-dimensional data to the low-dimensional space description, which will greatly improve the fault diagnosis efficiency.

A. APPLICATION OF LLE

Constant deviation of the telemetry data for pitch angular velocity, it indicates that the attitude sensor drifts, and the normal value deviation fault occurs in the 500~530 data points of the pitch angular velocity in the telemetry data. The fault form $\dot{\theta}_{out} = \dot{\theta}_0 + \Delta\dot{\theta}_f$, where $\Delta\dot{\theta}_f$ is the constant value deviation fault, the size is about 0.16°/s. The pre-processed data and the data obtained after applying LLE dimension reduction are shown in Figure 11. The results of fault detection using statistics are shown in Figure 12.

The detection results of T^2 and SPE under constant deviation are shown in Figure 12. When an abnormality occurs, the statistics T^2 and SPE jump beyond the corresponding control limit, and after the abnormality disappears, the statistics return to the control limit again. In order to quantify the detection effect, different statistics of FAR and MAR under constant deviation under Table 2. The statistical results show that for the constant deviation, both the false

TABLE 2. Different statistics of FAR and MAR under constant deviation.

LLE	FAR	MAR
T^2	6.1232%	10.2212%
SPE	3.7424%	0%

positive rate and the false negative rate meet the engineering requirements.

B. APPLICATION OF SLLE

LLE algorithm is a batch processing method. Although it can be applied to online data feature extraction, once the training data is given, the mapping matrix is fixed, and it is difficult to ensure the accuracy of online data dimensionality reduction. Over time, telemetry data characteristics of some parameters will inevitably change or drift, which means that the updated new sample data will affect the internal geometry of the original training data. At this time, the mapping matrix will be used to solve the sample low-dimensional space coordinates. There will be a large deviation, and it is necessary to consider updating the original training database.

For the above pre-processed telemetry data, the SLLE algorithm is applied to continuously update and supplement the original database through online data. Since d is an intrinsic property of the data, d does not change if the parameter type is unchanged. The neighborhood point k needs to be adjusted. Here, $k = 12$, which is much less than the number
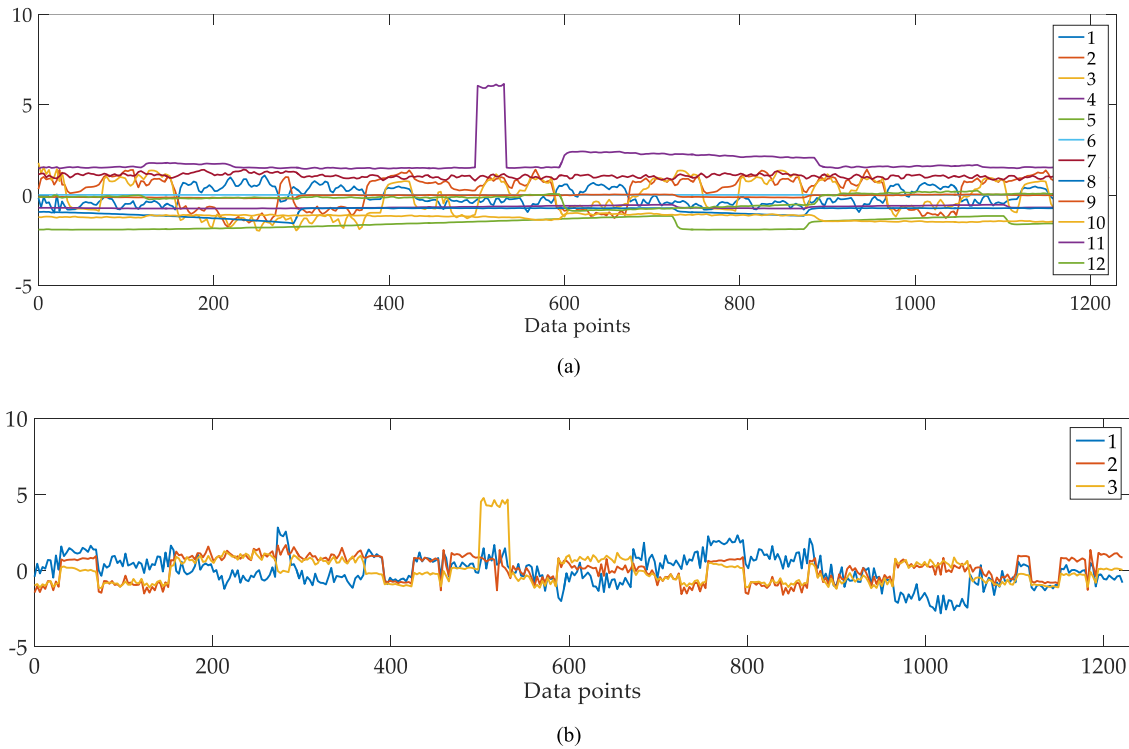
(a)

(b)

FIGURE 11. Preprocessed data and dimensionality reduction results under constant deviation: (a) Preprocessed data under constant deviation: 1,2,3- magnetic torque current; 4,5,6-flywheel torque; 7,8,9-fiber optic gyro angular velocity; 10,11,12-attitude angular velocity. (b) Dimensionality reduction results under constant deviation.
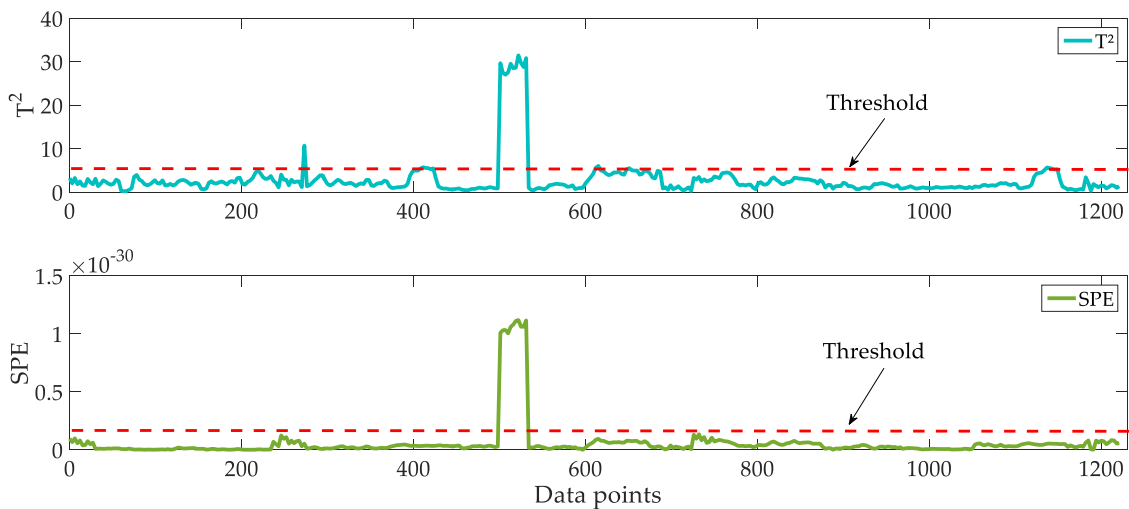

FIGURE 12. Test results of T2 and SPE under constant deviation.

of neighborhood points of the LLE algorithm, which greatly reduces the computational complexity. The dimensionality reduction result is shown in Figure 13.

The statistical test results based on the SLLE method under constant deviation are shown in Figure 14. When the constant deviation occurs, the statistic will jump beyond the control limit. After the constant deviation disappears, the statistic returns to the safe limit. Comparing the results of different

detection methods, it can be seen that the detection result based on SLLE algorithm is more ideal, and the detection results of T^2 and SPE are better than the constant deviation of Figure 12. In order to quantify the detection effect, different statistics of FAR and MAR under constant deviation under Table 3.

The test results show that for the same fault, the SLLE-based satellite attitude control system fault detection
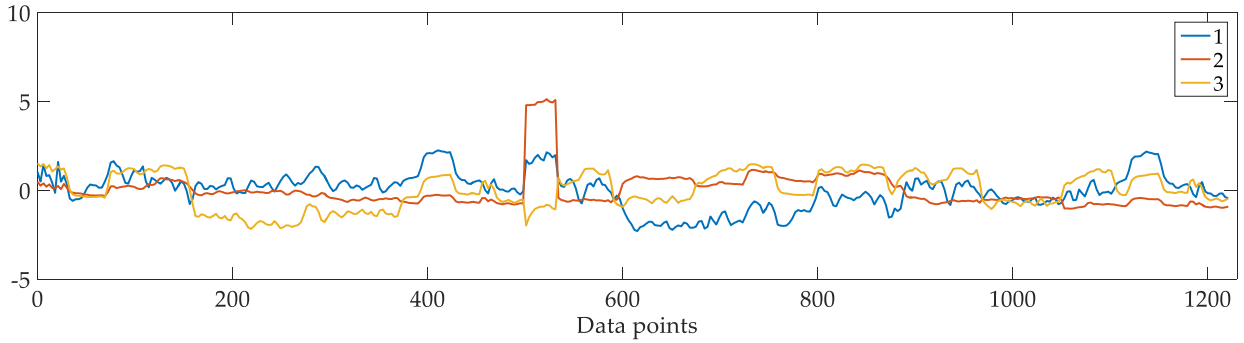
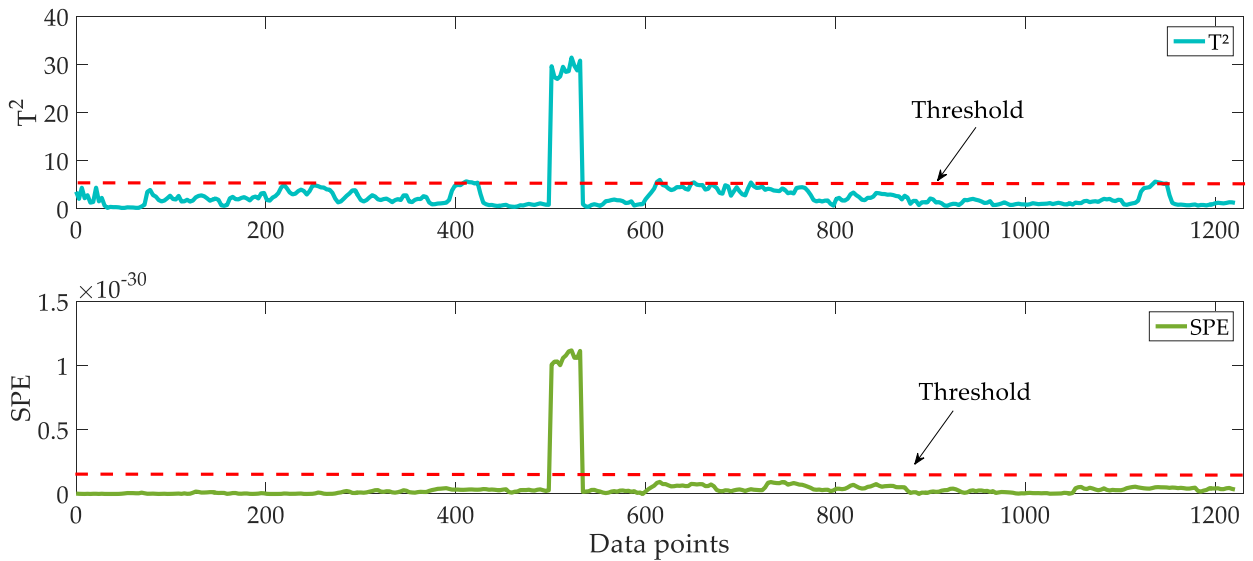**FIGURE 13.** Dimensionality reduction results under constant deviation.

FIGURE 14. Test results of T2 and SPE under constant deviation.

TABLE 3. Different statistics of FAR and MAR under constant deviation.

SLLE	FAR	MAR
T^2	2.5102%	0%
SPE	1.7894%	0%

algorithm is better than the LLE based fault detection effect. The statistics of each statistic fault detection result are shown in Table 3. The statistical results can quantitatively understand the fault detection effect of the two methods. The fault detection FAR and MAR based on SLLE are between 0% and 2.51%, while the fault detection FAR and MAR based on LLE are above 5%. The comparison result is sufficient to display SLLE. Both methods provide research ideas and theoretical references for engineering applications requiring general accuracy.

VII. CONCLUSION
In this paper, we aim at the problem that non-linear high-dimensional data is difficult to analyze, the research on

data dimension reduction and feature extraction based on LLE and SLLE is carried out. Taking Luojia1-01 satellite attitude-controlled telemetry data as the research object, different algorithms are used to extract high-dimensional data features, and combined with statistical *SPE* and T^2 to design fault detection scheme, and finally through Luojia1-01 satellite telemetry data simulation, the effectiveness of two schemes in this paper is verified. The results show that the fault detection method based on SLLE reduces the FAR by approximately 3% and the MAR by approximately 10% compared with LLE. This method effectively improves the detection capability of the anomalous state of Luojia1-01 satellite and has certain engineering application value.

REFERENCES

[1] *The Luojia-1A Scientific Experimental Satellite Was Successfully Launched*. Accessed: Aug. 2, 2018. [Online]. Available: http://www.lmars.whu.edu.cn/index.php/en/researchnews/2169.html

[2] G. Zhang, X. Guo, D. Li, and B. Jiang, "Evaluating the potential of LJ1-01 nighttime light data for modeling socio-economic parameters," *Sensors*, vol. 19, p. 1465, Mar. 2019.

[3] G. Zhang, L. Li, Y. Jiang, X. Shen, and D. Li, "On-orbit relative radiometric calibration of the night-time sensor of the Luojia1-01 satellite," *Sensors*, vol. 18, no. 12, p. 4225, 2018.

[4] X. Zhong, Z. Su, G. Zhang, Z. Chen, Y. Meng, D. Li, and Y. Liu, "Analysis and reduction of solar stray light in the nighttime imaging camera of Luojia-1 satellite," *Sensors*, vol. 19, no. 5, p. 1130, 2019.

[5] S.-L. Zhao and Y.-C. Zhang, "SVM classifier based fault diagnosis of the satellite attitude control system," in *Proc. Int. Conf. Intell. Comput. Technol. Automat.*, Oct. 2008, pp. 907–911.

[6] X. Ding, L. Guo, and T. Jeinsch, "A characterization of parity space and its application to robust fault detection," *IEEE Trans. Autom. Control*, vol. 44, no. 2, pp. 337–343, Feb. 1999.

[7] S. Lin and Z. Ying, "Fault diagnosis of navigation satellite attitude control system based on data-driven combined with artificial intelligence," in *Proc. China Satell. Navigat. Conf.*, 2010, pp. 123–136.

[8] L. Li, L. Ma, and K. Khorasani, "A dynamic recurrent neural network fault diagnosis and isolation architecture for satellite's actuator/thruster failures," in *Proc. Int. Symp. Neural Netw.*, 2005, pp. 574–583.

[9] N. Tudoroiu and K. Khorasani, "Fault detection and diagnosis for satellite's attitude control system (ACS) using an interactive multiple model (IMM) approach," in *Proc. IEEE Conf. Control Appl.*, Aug. 2005, pp. 1287–1292.

[10] N. Meskin and K. Khorasani, "Fault detection and isolation in a redundant reaction wheels configuration of a satellite," in *Proc. IEEE Int. Conf. Syst., Man Cybern.*, Oct. 2007, pp. 3153–3158.

[11] T. Jiang, K. Khorasani, and S. Tafazoli, "Parameter estimation-based fault detection, isolation and recovery for nonlinear satellite models," *IEEE Trans. Control Syst. Technol.*, vol. 16, no. 4, pp. 799–808, Jul. 2008.

[12] N. Tudoroiu, E. Sobhani-Tehrani, and K. Khorasani, "Interactive bank of unscented Kalman filters for fault detection and isolation in reaction wheel actuators of satellite attitude control system," in *Proc. IEEE 32nd Annu. Conf. Ind. Electron.*, Nov. 2006, pp. 264–269.

[13] B. Jiang, J. L. Wang, and Y. C. Soh, "An adaptive technique for robust diagnosis of faults with independent effects on system outputs," *Int. J. Control*, vol. 75, no. 11, pp. 792–802, 2002.

[14] B. Jiang, M. Staroswiecki, and V. Cocquempot, "Fault accommodation for nonlinear dynamic systems," *IEEE Trans. Autom. Control*, vol. 51, no. 9, pp. 1578–1583, Sep. 2006.

[15] T. Wang, Y. Cheng, B. Jiang, and R. Qi, "Fault detection based on finite impulse response adaptive filter for satellite attitude control systems," in *Proc. Control Decis. Conf.*, May/Jun. 2014, pp. 209–213.

[16] T. Yairi, Y. Kawahara, R. Fujimaki, Y. Sato, and K. Machida, "Telemetry ming: A machine learning approach to anomaly detection and fault diagnosis for space system," in *Proc. 2nd IEEE Int. Conf. Space Mission Challenges Inf. Technol.*, 2006, pp. 466–473.

[17] T. Yang, B. Chen, Y. Gao, J. Feng, H. Zhang, and X. Wang, "Data mining-based fault detection and prediction methods for in-orbit satellite," in *Proc. 2nd Int. Conf. Meas., Inf. Control*, Aug. 2013, pp. 805–808.

[18] Y. Gao, T. Yang, N. Xing, and M. Xu, "Fault detection and diagnosis for spacecraft using principal component analysis and support vector machines," in *Proc. 7th IEEE Conf. Ind. Electron. Appl. Conf.*, Jul. 2012, pp. 1984–1988.

[19] R. Fujimaki, T. Yairi, and K. Machida, "An approach to spacecraft anomaly detection problem using kernel feature space," in *Proc. 11th ACM SIGKDD Int. Knowl. Discovery Data Mining Conf.*, 2005, pp. 401–410.

[20] L. Zheng, J. Guang, and T. S. Han, "Fluctuation feature extraction of satellite telemetry data and on-orbit anomaly detection," in *Proc. Prognostics Syst. Health Manage. Conf. (PHM-Chengdu)*, Oct. 2016, pp. 1–5.

[21] D. de Ridder, O. Kouropteva, O. Okun, M. Pietikäinen, and R. P. W. Duin, "Supervised locally linear embedding," in *Proc. Artif. Neural Netw. Neural Inf. Process.*, vol. 2714, 2003, pp. 333–341.

[22] T. Wang, Y. Cheng, B. Jiang, R. Qi, and H. Qi, "Feature extraction and fault detection based on telemetry data for satellite TX-I," in *Proc. IEEE Chin. Guid., Navigat. Control Conf.*, Aug. 2014, pp. 1174–1179.

ZHI QU was born in Yantai, Shandong, China, in 1993. He received the B.S. degree from Changchun University, Changchun, China, in 2016. He is currently pursuing the Ph.D. degree with the Changchun Institute of Optics, Fine Mechanics and Physics, Chinese Academy of Sciences, Changchun.

His research interests include satellite attitude dynamics and control, and satellite fault-tolerant control.
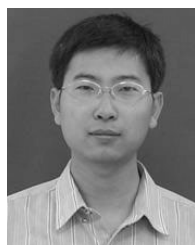
KAI XU received the B.E. degree from Jilin University, Changchun, China, in 2004, and the Ph.D. degree from the Changchun Institute of Optics, Fine Mechanics and Physics, Chinese Academy of Sciences, Changchun, in 2009.

He is currently a Professor with the University of Chinese Academy of Sciences. His research interests include satellite's overall design and satellite attitude dynamics and control.

ZHIGANG CHEN received the B.E. degree from the Changchun University of Technology, Changchun, China, in 2011, and the master's degree from the College of Communications Engineering, Jilin University, Changchun, in 2016.

He is currently with Chang Guang Satellite Technology Company Ltd. (CGSTL). His research interests include satellite attitude and orbit control system design.

XIN HE received the Ph.D. degree from the Changchun Institute of Optics, Fine Mechanics and Physics, Chinese Academy of Sciences, Changchun, in 1991.

He is currently a Professor with the University of Chinese Academy of Sciences. His research interests include research on image processing and pattern recognition.

YANHAO XIE received the B.S. and M.S. degrees in astronautic engineering and mechanics from the Harbin Institute of Technology, in 2015 and 2017, respectively. He became an Engineer. His main research interests include satellite attitude control system modeling and simulation, satellite mission planning, and satellite shooting space target.
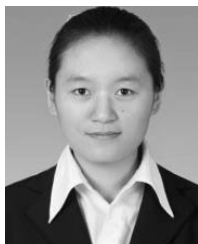
MENGMENG LIU received the M.S. degree in control engineering from the Harbin Institute of Technology, Harbin, China, in 2016.

Her main research interest includes multi-spacecraft system distributed attitude cooperative tracking control.

SHUANGXUE HAN was born in Inner Mongolia. She received the bachelor's degree from the Harbin Engineering University, in 2013, and the master's degree in aeronautical engineering from Northwest Polytechnic University, in 2016. She is currently with Chang Guang Satellite Technology Company Ltd., responsible for dynamics modeling and simulation of aircraft.

• • •

FENG LI received the B.S. and M.S. degrees from Harbin Engineering University, in 2011 and 2013, respectively.

His main research interests include satellite attitude and orbit control.